

Ab initio compressive phase retrieval

Stefano Marchesini

*Centre for Free-Electron Laser Science, DESY,
Notkestrasse 85, 22607 Hamburg, Germany. and*

*Permanent address: Advanced Light Source, Lawrence Berkeley National Laboratory,
1 Cyclotron Rd, Berkeley CA 94720, USA. e-mail: smarchesini@lbl.gov*

Any object on earth has two fundamental properties: it is finite, and it is made of atoms. Structural information about an object can be obtained from diffraction amplitude measurements that account for either one of these traits. Nyquist-sampling of the Fourier amplitudes is sufficient to image single particles of finite size at any resolution. Atomic resolution data is routinely used to image molecules replicated in a crystal structure. Here we report an algorithm that requires neither information, but uses the fact that an image of a natural object is compressible. Intended applications include tomographic diffractive imaging, crystallography, powder diffraction, small angle x-ray scattering and random Fourier amplitude measurements.

© 2022 Optical Society of America

OCIS codes: 100.5070 100.3190

1. Intro

In a standard imaging system, light scattered from an object forms a diffraction pattern which encodes information about the object Fourier components. A lens recombines the scattered rays so that they interfere correctly to form an image: it performs an inverse Fourier transform of the diffraction pattern to convert Fourier (reciprocal) representation of the object into real space information.

At visible wavelengths, aberration-free lenses can provide diffraction limited images within a limited depth of field. Smaller wavelengths offer much higher resolutions by reducing the diffraction limit. X-rays also offer the ability to penetrate through thick objects and allow one to examine elemental, chemical, or magnetic information by exploiting mechanisms such as resonant X-ray scattering. Unfortunately, diffraction limited optics are harder to come by for X-rays, whose paths are difficult to manipulate. For higher resolutions, the optics need to cope with light scattered to high angles. Building such optics is a difficult technical challenge. Currently, focal widths of tens of nanometers are achievable, but lenses capable of atomic resolution are so far well beyond reach.

Diffraction and scattering experiments overcome this problem by eliminating the need for any optics. The concept is to record the scattering pattern created by an object and perform the re-interference normally done by a lens numerically instead. Since no optical elements are used, aberration free images may be obtained with resolutions limited in principle only by the maximum momentum transfer which can be achieved. However, the resulting image is additionally limited by the computer's ability to recover the entire image from incomplete Fourier information and loss of phase information. The intimate relationship between the phase-front and

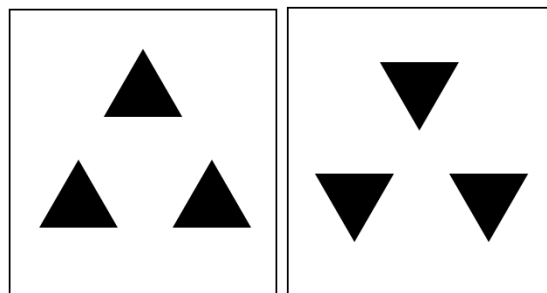


Fig. 1. Simple homometric objects[1], with the same Fourier magnitude, are composed by the convolution between two non-centrosymmetric objects.

the direction of propagation seems to suggest that the task of recombining x-rays back at the sample position would seem hopeless. It is not so under a surprisingly small set of conditions.

The importance of fine sampling of the diffraction pattern intensity was recognized at an early stage in x-ray crystallography. The observation that Bragg diffraction undersamples the diffracted intensity pattern [2, 3] was followed by the demonstration that the solutions to Nyquist sampled diffraction patterns are almost always unique [4, 5, 6, 7] (although one could easily make up examples where this is not the case -see Fig. 1).

These ideas, along with the development of powerful light sources, producing collimated beams of coherent x-rays, enabled the development of coherent x-ray diffraction microscopy [8] (aka lensless or diffractive imaging). This technique aims at imaging, through coherent illumination, Fourier amplitude measurements and adequate sampling, macroscopic objects such as entire cellular organisms [9], or nanoporous aerogel structures [10]. See

[11] for a review.

Diffraction microscopy solves the phase problem using increasingly sophisticated algorithms based on the support constraint, which assumes adequate sampling. The object being imaged is limited within a support region S :

$$\rho(\mathbf{r}) = 0, \text{ if } \mathbf{r} \notin S. \quad (1)$$

The sampling conditions required to benefit from the support constraint have limited the adoption of projection algorithms to other experimental geometries that allow only for sub-Nyquist sampling, most notably Bragg sampling from periodic crystalline structures.

Modern sampling theory however, tells us that that Nyquist sampling conditions dictated by the support are the worst case scenario for an arbitrary object. In other words, Shannon was a pessimist: he did not account for the signal structure. Compressive sensing theory tells us that the number of measurements are dictated by the signal structure rather than it's length. By structured we mean that the signal has only a few non-zero coefficients when represented in terms of some basis, or can be well approximated well by a few non zero coefficients: they can be described in terms of a few atoms, a few stars, a few wavelet coefficients, or possibly a few protein folds.

In other words, an object of interest is often sparse or concentrated in a small number of non-zero coefficients in a well chosen basis, i.e. it can be compressed with no or almost no loss of information. The meanings of "well-chosen" and "of interest" are slightly circular: A basis is well-chosen if it succinctly describes a signal of interest; likewise, a signal is of interest if it can be described with just a handful of basis elements.

Since we do not know where these few terms are located, conventional wisdom would indicate that one has to first measure the full sample at the desired resolution, since overlooking an important component of a signal seems almost inevitable if the whole haystack isn't thoroughly searched over. There would seem to be no alternative to processing each signal in its entirety before we can compress it and store only the desired information (such as the location of the atoms in a molecule).

But a new theory of "compressive sampling" has shown how an image of interest or structured signals generally can be reconstructed, exactly, from a surprisingly small set of direct measurements. Candès and colleagues [12] have defined a notion of "uniform uncertainty" that guarantees, with arbitrarily high probability, an exact solution when the signal is sparse and a good approximation when it is compressible or noisy. Their uniform uncertainty condition is satisfied, among others, by Fourier measurements of a sparse real space object.

The question of whether modern sensing theory is applicable to Fourier amplitude measurements was first raised by Moravec, Romberg and Baraniuk [13] who provide an upper bound sampling condition for the successful retrieval of a sparse signal autocorrelation, and discuss other conjectures with far reaching consequences for low-resolution undersampled phase retrieval. Since the

theory is relatively new and not widely known to the phase retrieval community, modern sampling theory is briefly reviewed.

2. A nonlinear sampling theorem

The notion that a diffraction pattern from a sparse object can be reconstructed at sub-Nyquist sampling is not entirely new. The so called "Direct methods" are routinely used for atomic resolution imaging of increasing complex molecular structures. Direct methods enforce the condition that the resulting molecule is composed of a finite number of atoms. The conditions for successful ab-initio phase retrieval using these methods are strict: it requires (1) atomic resolution and (2) about 5 strong peaks per atom. Condition (2) means that the algorithms do not scale well with a large number of atoms since the number of strong reflections decreases rapidly with the number of atoms.

Here we look for an alternative answer from modern sampling theory.

Suppose that one collects an incomplete set of frequency samples (amplitude and phase) of a discrete signal $\rho(r)$ of length N . The goal is to reconstruct the full signal ρ given only K samples in the Fourier domain where the "visible frequencies" are a subset Ω (of size K) of the set of all frequencies $\{0, \dots, N\}$.

At first glance, solving the underdetermined system of equations appears hopeless, as it is easy to make up examples for which it clearly cannot be done. But suppose now that the signal ρ is compressible, meaning that it essentially depends on a number of degrees of freedom which is smaller than N . Then in fact, accurate and sometimes exact recovery is possible by solving a simple convex optimization problem.

Theorem 2.1. (*Candes Romberg and Tao [12]*): *Assume that ρ is n_a -sparse, (e.g. n_a atomic charges in real space with N resolution elements), and that we are given K Fourier coefficients with frequencies selected uniformly at random. Suppose that the number of observations obeys $K < Cn_a \log N$. Then minimizing ℓ_1 reconstructs ρ exactly with overwhelming probability. In particular, writing $C = 22(\delta + 1)$, then the probability of success exceeds $1 - N^{-\delta}$.*

The theorem shows that a simple convex minimization will find the exact solution without any knowledge about the support, the number of nonzero coordinates of r , their locations, and their amplitudes which we assume are all completely unknown a priori.

Following [12] we formulate this more explicitly. The algorithm that optimizes the ℓ_1 norm:

$$\min |\rho|_1 \text{ subject to } \mathcal{F}\rho = F, \{\mathbf{k} \in \Omega\}; \quad (2)$$

$$|\rho|_1 = \sum |\rho(x)| \quad (3)$$

will find the solution with the correct answer without knowing the support S ($S =$

{1 if $|\rho_0(x)| > 0$, 0 otherwise}), nor the number of non-zero elements $\|\rho_0\|_0$ ($\|\rho_0\|_0 = \sum S$).

In addition, another remarkable result, is that the concept of “atomicity” in real space is generalized to sparsity in other basis. We can use, instead of a dictionary of point atoms, a dictionary of curves, beams, or a basis that describes protein folds using a few terms. Finally, since the equation above does not depend strongly on N , the number of resolution elements or the basis, we can choose redundant basis, with more terms than real space resolution elements if it helps to describe the object with fewer terms.

The only requirement is to be able to find the minimum of $\|\rho\|_1 = \sum |\rho(\mathbf{x})|$. These results have already been applied to a number of imaging techniques, but they require amplitude and phase of the Fourier coefficients. The question that we try to address here is: what are the implications to the inversion problem of Fourier magnitude only recordings?

The following theorem gives an upper bound:

Theorem 2.2. (*Moravec, Romberg and Baraniuk [13]*): *Assume that ρ is n_a -sparse, then it can be recovered exactly from a reduced number of random Fourier magnitude measurements $K > Cn_a^2 \log(4M/n_a^2)$.*

The theorem is based on the fact that the autocorrelation of an n_a -sparse object is at most n_a^2 sparse. The authors also point out that n_a^2 sparse is worst case scenario. If the object is connected, then the sparsity of the autocorrelation grows linearly, instead of quadratically, with the object support to twice the object size. In summary, this theorem provides an upper bound for the exact recovery of the object autocorrelation for an arbitrary but finite object, as well as from sub-sampled data for an object made of a few atoms.

The important question then is: does a typical geometry used in x-ray diffraction satisfy the conditions required to enable the full recovery of the object’s autocorrelation? One of the keys to compressive sensing is the role played by randomness in the data acquisition (from the Uniform Uncertainty Principle[12]). Does a Bragg geometry satisfy these conditions? In this section we explore the possibility that various sampling geometries satisfy the condition for compressive recovery of the autocorrelation.

We simulate an object of n_a atoms, and attempt to recover the full autocorrelation from a subset of Fourier amplitude measurements. The optimization problem can be stated as follows:

$$\min |\rho|_1 \text{ subject to } |\mathcal{F}a|^2 = I_k \quad (4)$$

where a is the autocorrelation of the object we are trying to reconstruct.

The problem setting was written within the SPARCO toolbox[14]. With the addition of radial averaging, the SPARCO toolbox provided the operators to simulate a general scattering experiment: a Fourier transform, and

a Fourier mask. The SPGL1 software [15] used here was able to converge quickly to a root. Various sampling conditions are explored in Fig. 2. We can see that random Fourier sampling and limited angle tomography satisfy the conditions for exact recovery, while Bragg sampling (sampling every other 2 Fourier components in each dimension) does not. However we are able to recover the aliased autocorrelation from a severely reduced number of measured Bragg reflections or even from radially averaged powder data (using an oblique unit cell which causes a reduced number of peak overlaps, in this case an average of 10 peak overlap over the same radial shell).

3. Compressive phase retrieval algorithms

Although results described above are encouraging, it is obvious that we can do better than that: we have not utilized the notion that the function that we have been trying to recover is itself the autocorrelation of an even sparser object. We therefore look for an algorithm that recovers a sparse object from subsampled Fourier amplitude measurements.

Though problems of this (non-convex) nature are difficult because only exhaustive algorithms can guarantee convergence, a variety of heuristics perform well in practice. We follow the notation described elsewhere [28] for projection algorithms.

A. Projection algorithms

The aim of projection algorithms is to find a signal that lies in the intersection of two constraint sets. The first set is that of the measured Fourier magnitudes. To compute the projector corresponding to the Fourier magnitude constraint, one first needs to propagate $\rho(\mathbf{r})$ to the data space by a Fourier transform \mathcal{F} , and then replace estimated amplitudes $|\tilde{\rho}|$ ($\tilde{\rho}(\mathbf{k}) = \mathcal{F}\rho(\mathbf{r})$) with the measured ones, and propagate back to real space. Formally, we incorporate the forward \mathcal{F} and inverse \mathcal{F}^{-1} Fourier transform in the operator defined in Fourier space $\tilde{\mathbf{P}}_m$:

$$\mathbf{P}_m = \mathcal{F}^{-1} \tilde{\mathbf{P}}_m \mathcal{F}, \quad (5)$$

and enforce the condition that the image Fourier magnitudes are equal to the measured ones. Using these transforms one simplifies the calculation of the projection which becomes an element-wise operation on each recovered Fourier component:

$$\tilde{\mathbf{P}}_m \tilde{\rho}(\mathbf{k}) = \sqrt{I(\mathbf{k})} \frac{\tilde{\rho}(\mathbf{k})}{|\tilde{\rho}(\mathbf{k})|}, \quad (6)$$

This projection requires each Fourier measurement to be sampled individually. In powder diffraction, partial coherent illumination, broadband illumination, the projection operator needs to be generalized. If one defines the averaging operator A , the generalization is as follows [30]:

$$\tilde{\mathbf{P}}_m \tilde{\rho}(\mathbf{k}) = \tilde{\rho}(\mathbf{k}) \sqrt{\frac{I(\mathbf{k}_A)}{A|\tilde{\rho}(\mathbf{k})|^2}}, \quad (7)$$

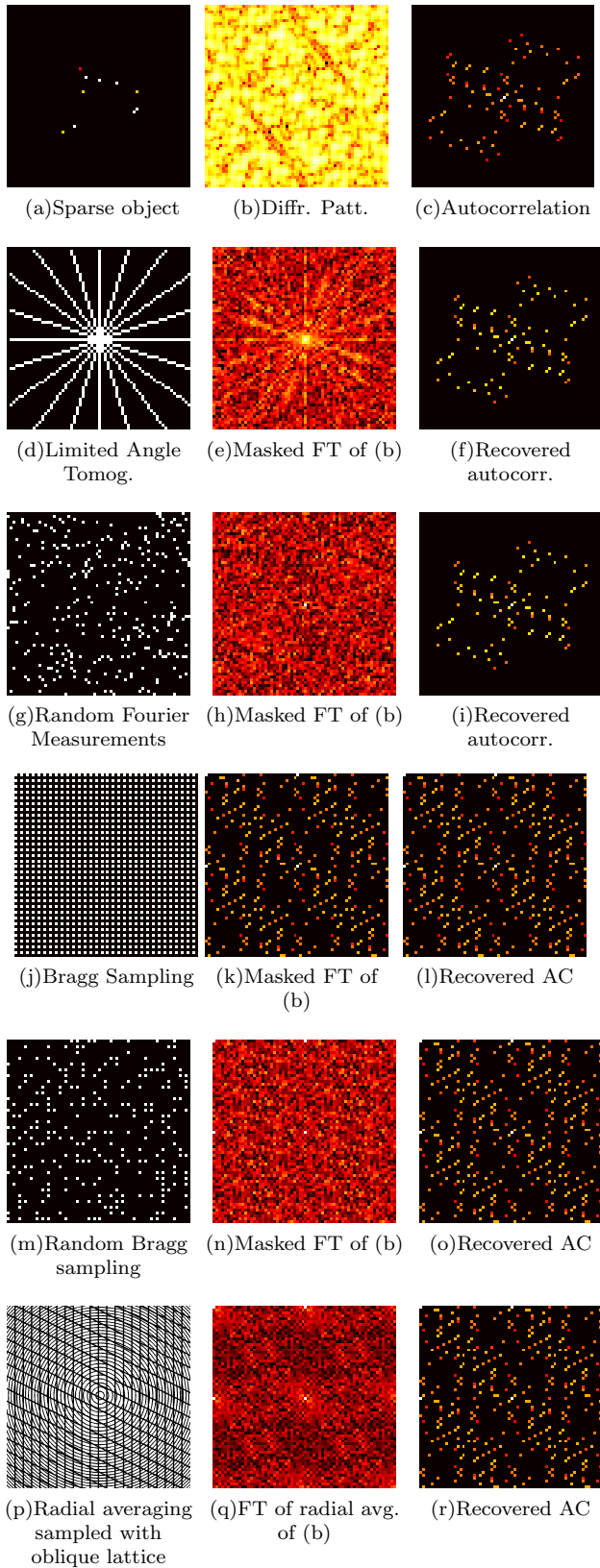


Fig. 2. **Recovering a sparse autocorrelation.** Top row: (a) Original object, (b) Fourier magnitude (c), autocorrelation. In the successive rows, Fourier mask (left), autocorrelation from masked Fourier amplitudes (center), recovered autocorrelation using ℓ_1 minimization (right). Fourier masks: (d) limited angles (g) random (j) Bragg (m) random Bragg (p) radial average -oblique unit cell.

where \mathbf{k}_A is the corresponding value of the intensity which $|\tilde{\rho}(\mathbf{k})|$ contributes to. Partial overlap can be analyzed using the Richardson-Lucy deconvolution [16, 17] of the intensities under square root (see also [18]). The second projector, used in diffractive imaging, is that of the support: $\mathbf{P}_s \rho(\mathbf{r}) = \{\rho(\mathbf{r}) \text{ if } \mathbf{r} \in S; 0 \text{ otherwise}\}$ that acts element-by-element to the real space basis.

While early experiments relied on low resolution imaging to determine the object support, the development of automated support refinement techniques [19] have enabled diffractive imaging to solve structures independently. Note that these SHRINKWRAP support finding techniques rely on the most compact (and sparse) object that satisfy the measurements.

B. Sparsifying algorithms

Since we do not know the support of our signal, we replace the projection onto the support set P_s with a variety of operators O known to promote sparsity in phase retrieval problems: thresholding, Sayre' squaring operator [20], and a soft thresholding operator that promotes sparsity through ℓ_1 optimization [34] (Moravec et al. suggest using the ℓ_1 norm as a constraint, but this is rarely known):

$$O_\tau x = \begin{cases} x & \text{if } |x| > \tau, \\ 0 & \text{otherwise.} \end{cases} \quad (8)$$

$$O_2 x = x^2, \quad (9)$$

$$O_{\ell_1} x = \begin{cases} x - \tau \frac{x}{|x|} & \text{if } |x| > \tau, \\ 0 & \text{otherwise.} \end{cases} \quad (10)$$

With slight abuse of notation, we use the same symbol for a projector, and define a reflector operator:

$$\mathbf{P}_{\tau,2,\ell_1} = \mathbf{O}_{\tau,2,\ell_1}; \mathbf{R}_{\tau,2,\ell_1} = 2\mathbf{O}_{\tau,2,\ell_1} - \mathbf{I};$$

The first most obvious algorithms are simple alternating type:

$$\rho^{(n+1)} = \mathbf{P}_m \mathbf{O}_{(\tau,\ell_1,2)} \rho^{(n)}$$

We note that the squaring method obtained by alternating the operators $\mathbf{P}_m \mathbf{O}_2 x$ is equivalent to the ‘‘tangent formula’’ of Direct methods, where the squaring operation equation in real space is performed directly in Fourier space through an autocorrelation. Remarkable improvements in the range of convergence has been obtained by increasing the step produced by these algorithms in real space by 2, using the reflector operator \mathbf{R} . The charge flipping algorithm replaces the thresholding operation by with an operator that moves twice as far:

$$\rho^{(n+1)} = \mathbf{P}_m \mathbf{R}_{(\tau,\ell_1,2)} \rho^{(n)}$$

In appendix we describe why it is superior to simple alternating projections.

Table 1. Summary of various algorithms

Algorithm	Iteration $\rho^{(n+1)} =$
ER	$\mathbf{P}_s \mathbf{P}_m \rho^{(n)}$
SF	$\mathbf{R}_s \mathbf{P}_m \rho^{(n)}$
HIO	$\begin{cases} \mathbf{P}_m \rho^{(n)}(\mathbf{r}) & \mathbf{r} \in S \\ (\mathbf{I} - \beta \mathbf{P}_m) \rho^{(n)}(\mathbf{r}) & \mathbf{r} \notin S \end{cases}$
DM	$\{\mathbf{I} + \beta \mathbf{P}_s [(1 + \gamma_s) \mathbf{P}_m - \gamma_s \mathbf{I}] - \beta \mathbf{P}_m [(1 + \gamma_m) \mathbf{P}_s - \gamma_m \mathbf{I}]\} \rho^{(n)}$
ASR	$\frac{1}{2} [\mathbf{R}_s \mathbf{R}_m + \mathbf{I}] \rho^{(n)}$
HPR	$\frac{1}{2} [\mathbf{R}_s (\mathbf{R}_m + (\beta - 1) \mathbf{P}_m) + \mathbf{I} + (1 - \beta) \mathbf{P}_m] \rho^{(n)}$
RAAR	$[\frac{1}{2} \beta (\mathbf{R}_s \mathbf{R}_m + \mathbf{I}) + (1 - \beta) \mathbf{P}_m] \rho^{(n)}$

However we are interested in an algorithm that is more general than this for reasons that will become apparent in the following section. In particular we need an algorithm that is robust against the relaxation of the positivity of the object, and the change of basis used to describe the object.

The algorithms tested include: HIO[22], SF[23], DM [24], HPR[25] and RAAR[26] (see [28] for a review). We tested algorithms based on these ideas for increasingly complex phase retrieval problems. A unit cell in a periodic system was filled with a limited number of atoms. First an algorithm has to be stable around the solution. If perturbed from the solution, it should go back or at least not diverge much from it. Perturbations tested included: distributed noise, ‘‘salt and pepper’’ noise and a single large extra charge added to the structure. Secondly, it should converge to the solution starting from an arbitrary set of phases for a large number of atoms n_a . For small n_a all but a handful of algorithms work, as n_a increases, it takes longer to converge, and one by one, various algorithms stop working. The best algorithm is the one that works with highest ratio between number of atoms and number of measurements.

Through these numerical tests, the following outperformed all others (fig. 3):

$$\begin{aligned} S_1 &= |\mathbf{P}_m \rho - \rho| > \tau_1, \\ S_2 &= \mathbf{P}_m \rho > 0 \\ \rho^{(n+1)} &= (S_1 \& S_2) (\mathbf{P}_m \rho^{(n)}) + (1 - S_1) (\rho^{(n)}) \\ &\quad - \beta \mathbf{P}_m \rho^{(n)}; \end{aligned} \quad (11)$$

where $>$ is intended as a relational operator, $S_{1,2}$ are binary masks. If positivity cannot be enforced, then $S_2 = 1$. From here on, this algorithm will be referred to as ESPRESSO, in honor of the compressed coffee.

4. Beyond atoms

The algorithms described perform remarkably well in case an object being imaged is sparse in real space,

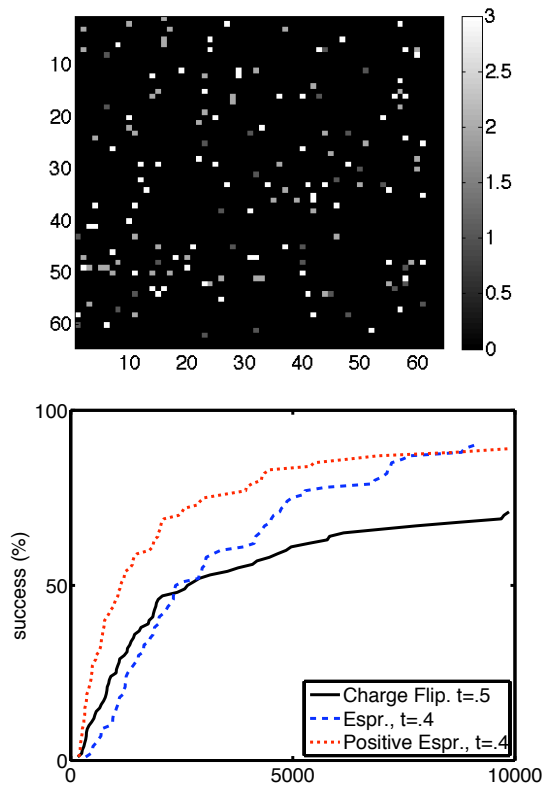


Fig. 3. **Recovering a sparse object in real space.** Comparison of various algorithms. Top: test unit cell, 64×64 resolution elements, 160 atoms of values ranging from 1 to 3 (arbitrary units). Bottom: success rate vs number of iterations, using the optimal threshold level ($\tau = .5$ for charge flipping, $.4$ for ESPRESSO); and $\beta = .5$.

namely that it is composed of a limited number of atoms. Object made of more than a few atoms, such as large macromolecules or biological cells, require a different approach.

Natural objects are often characterized by the fact that they are compressible in some basis. Everyone is familiar with the fact that images of millions of pixels can be saved with nearly indistinguishable accuracy at a small fraction of the initial image size. In other words, natural objects can often be accurately described in terms of only a few non-zero coefficients in some basis.

Moravec et al.[13] conjecture that compressive methods for phase retrieval could be applicable in a basis other than the real space. Here we set out to test this conjecture for the crystallographic phase problems with the ESPRESSO algorithm. Will all basis work? not if they are too localized in Fourier space, as preliminary tests with curvelets [31] seem to suggest.

The problem in this test is to recover a Schepp-Logan phantom test object. As in many tomographic settings, we seek to sparsify the the gradient of the object.

The discrete gradient is obtained by simple matrix op-

erations. One defines a two-dimensional matrix D_x of the same size as ρ , with the first two elements equal to -1 and +1 respectively, and the rest of the elements equal to 0. The discrete derivative is obtained by a simple convolution between the object and this matrix: $\partial_x \rho(\mathbf{r}) = D_x * \rho(\mathbf{r})$. Convolution becomes a product in Fourier space, where we define the discrete Fourier transform $\tilde{D}_x = \mathcal{F}D_x$: $\partial_x \rho = \mathcal{F}^{-1}(\tilde{D}_x \tilde{\rho})$. Similar arguments apply for the other direction. We define the matrix $D_y = D_x^T$ as the transpose of D_x .

The inverse operation used to recover the object from the compressed gradient values $(\partial_x \rho, \partial_y \rho)$ was the following pseudoinverse:

$$\rho = \mathcal{F}^{-1} \frac{\tilde{D}_x^\dagger \mathcal{F} \partial_x \rho + \tilde{D}_y^\dagger \mathcal{F} \partial_y \rho}{\tilde{D}_x^\dagger \tilde{D}_x + \tilde{D}_y^\dagger \tilde{D}_y + \varepsilon}, \quad (12)$$

with ε a regularization term. Once we have obtained the gradient, $[\partial_x, \partial_y] \rho$, we apply the Espresso algorithm in this space, trying to compress the gradient. The norm used was $\sqrt{|\partial_x \rho|^2 + |\partial_y \rho|^2}$:

$$S_1 = \sqrt{|\partial_x \mathbf{P}_m \rho - \rho|^2 + |\partial_y \mathbf{P}_m \rho - \rho|^2} > \tau_1,$$

$$S_2 = \sqrt{|\partial_x \mathbf{P}_m \rho|^2 + |\partial_y \mathbf{P}_m \rho - \rho|^2} > \tau_2,$$

$$\begin{aligned} \partial_x \rho^{n+1} &= (S_1 \& S_2)(\partial_x \mathbf{P}_m \rho^n) + (1 - S_1)(\partial_x \rho^n) - \beta \partial_x \mathbf{P}_m \rho^n, \\ \partial_y \rho^{n+1} &= (S_1 \& S_2)(\partial_y \mathbf{P}_m \rho^n) + (1 - S_1)(\partial_y \rho^n) - \beta \partial_y \mathbf{P}_m \rho^n; \end{aligned}$$

although the two gradient components could be treated separately, each with their own supports $S_{1,2}$.

Examples are shown in Fig. 4, where different masks are applied to the Fourier data: Full sampling, missing central region due to the beamstop, limited angles of tomographic datasets, Bragg sampling, and radially averaged powder data. Notably, the periodic crystal symmetry is ‘‘discovered’’ by sampling the diffraction pattern at the Bragg condition. In the case of powder diffraction, with an average of 20 overlaps per sampled point, the algorithm is still able to recover the outline of the object, or the dominant terms contributing to the gradient. The unit cell used for calculating the radial average was oblique, to reduce some peak overlaps. In each case the threshold is defined dynamically: $\tau = 2\sigma$, with $\sigma = rms(|\rho - \mathbf{P}_m \rho|)$.

5. Conclusions

The revolutionary findings of compressive sensing have shown how severely incomplete data can be used to recover both sparse and compressible signals from Fourier amplitude and phase measurements. This paper discusses its implications for the phase retrieval problem, namely that one does not need to assume a finite signal bandwidth, nor atomic resolution. A new algorithm for compressive phase retrieval has been proposed. It outperforms existing algorithms for atomic resolution data, and can be applied at arbitrary resolution to crystal diffraction, provided that the sample is compressible in some

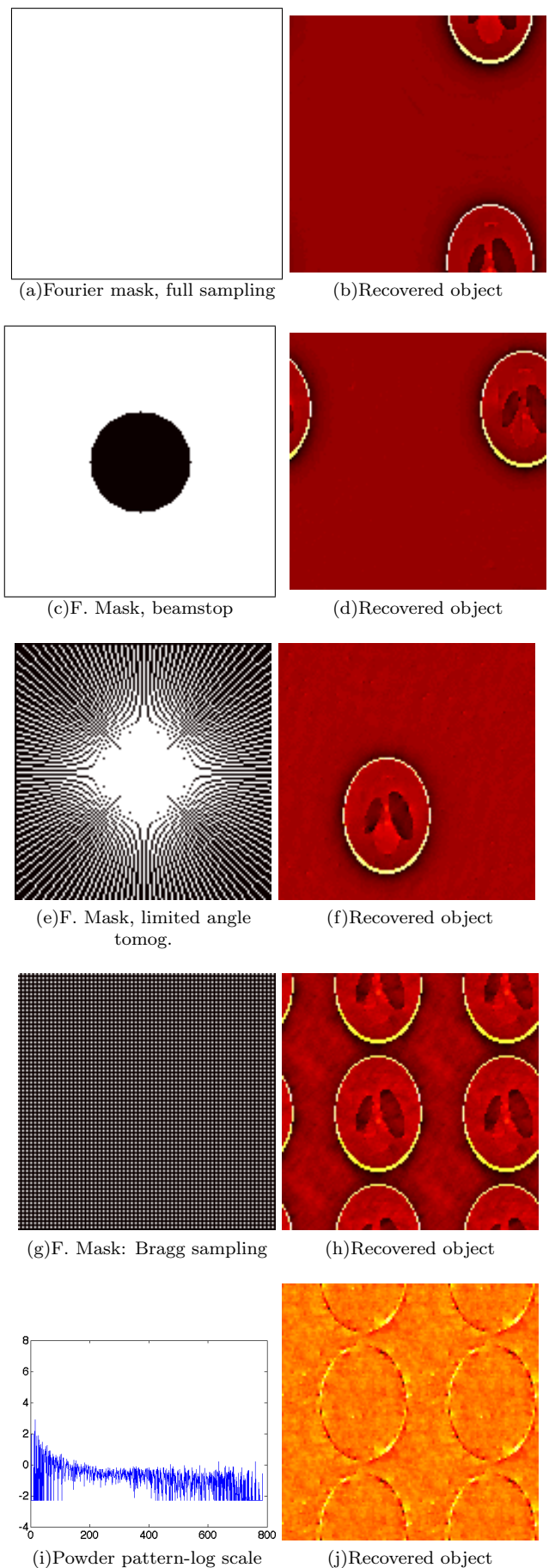


Fig. 4. **Recovering an object without atomic resolution.** Shepp-Logan phantom is embedded into a 128×128 image. Left: Fourier mask, Right: reconstruction. (a)-(b): Full sampling. (c)-(d) Beam stop. (e)-(f)

basis. Optimization of the parameter β on the fly at each iteration [32], promises to further improve this algorithm and will be subject of future work. The search for the optimal sparsifying basis and improved compressive algorithms promises to revolutionize low resolution phasing in X-ray diffraction.

ACKNOWLEDGMENTS This work was performed under the auspices of the U.S. Department of Energy by the Lawrence Berkeley National Laboratory under Contract No. W-7405-EEG-48 and the Director, Office of Energy Research. Part of this work was done while visiting the Center for Free Electron Lasers at DESY. Motivation for this work is due to the serial crystallography project of J. C. H. Spence et al., and recent experimental results by D. Shapiro et. al., as well as the diffractive imaging program at the Advanced Light Source. Inspiration for this work is due to discussions with C. Yang at the computational research division of Lawrence Berkeley Lab.

Appendix A: Charge flipping

Take a known object with charge density distribution $\rho(\mathbf{r})$, with Fourier amplitude $|\tilde{\rho}(\mathbf{k})| = \sqrt{I(\mathbf{k})}$. We first look at perturbations from the solution. If we add a random noise distribution a with root mean square (r.m.s.) $\sigma < \min(\rho : \rho > 0)$, a simple threshold will be able to isolate the signal $\rho > \sigma$ from the noise. As the noise grows, an increasing large percentage of noise will survive the thresholding operation and the thresholding algorithm will stagnate at first local minimum it encounters. At low perturbation levels, a simple thresholding operation is the obvious and effective answer. Flipping components below a threshold, rather than setting them to zero would just flip sign within a first order term, and at best remove second order $O(a^2/|\rho|)$ contributions to the noise a . We consider ‘‘salt and pepper’’ noise $a = \sum_{i=1}^s a_i^s \delta(x - x_i)$ with a few s terms, such as if we displaced a small percentage of the peaks from the correct answer). For simplicity, let us consider just a single charge a in x_0 :

$$\rho' = \rho + a\delta(x - x_0); \quad (\text{A1})$$

We enforce the measured data by applying the Fourier magnitude projector to the current guess $\tilde{\rho}' = \mathcal{F}\rho' = \tilde{\rho} + ae^{ikx_0}$:

The projection is performed by Fourier transforming $\tilde{\rho}' = \mathcal{F}\rho'$, and enforcing the Fourier magnitude:

$$\begin{aligned} \tilde{P}_m \tilde{\rho}' &= \sqrt{\frac{I}{|\tilde{\rho}'|^2}} \tilde{\rho}' \\ &= \sqrt{\frac{I}{|\tilde{\rho}|^2}} \frac{\tilde{\rho} + ae^{ikx_0}}{\sqrt{1 + \frac{\tilde{\rho}^*}{|\tilde{\rho}|^2} ae^{ikx_0} + \frac{\tilde{\rho}}{|\tilde{\rho}|^2} a^* e^{-ikx_0} + \frac{|a|^2}{|\tilde{\rho}|^2}}} \end{aligned}$$

using Taylor series $\frac{1}{\sqrt{1+x}} = 1 - \frac{1}{2}x + \frac{3}{8}x^2$:

$$\begin{aligned} &= (\tilde{\rho} + ae^{ikx_0}) \left(1 - \frac{1}{2} \frac{\tilde{\rho}^*}{|\tilde{\rho}|^2} ae^{ikx_0} - \frac{1}{2} \frac{\tilde{\rho}}{|\tilde{\rho}|^2} a^* e^{-ikx_0} + O(a^2) \right) \\ &= \tilde{\rho} + \frac{1}{2} ae^{ikx_0} - \frac{1}{2} \frac{\tilde{\rho} \tilde{\rho}^*}{|\tilde{\rho}|^2} ae^{ikx_0} + O(a^2) \\ &= \tilde{\rho} + \frac{1}{2} ae^{ikx_0} - \frac{1}{2} a^* F(x_0) + O(a^2) \end{aligned}$$

with $F(x_0) = \frac{\tilde{\rho}}{\tilde{\rho}^*} e^{-ikx_0}$. The term $\frac{\tilde{\rho}}{\tilde{\rho}^*}$ has a rapidly oscillating phase, and diffuses half of the charge a everywhere in the unit cell through the function $f = \mathcal{F}^{-1}F$. At first order in a one obtains:

$$\mathbf{P}_m \rho' = \rho + \frac{1}{2} a \delta(x - x_0) - \frac{1}{2} a^* f(x_0) + O(a^2) \quad (\text{A2})$$

with $f(x_0)$ being distributed over the unit cell. Since the charge is reduced only by half, we could try moving twice as far, instead of moving from ρ to $\mathbf{P}_m \rho$ by a step $I - \mathbf{P}_m$, using a reflector $\mathbf{R} = 2\mathbf{P} - \mathbf{I}$ to:

$$\mathbf{R}_m \rho' = \rho - a^* f(x_0) + O(a^2) \quad (\text{A3})$$

Suppose the threshold only picks up the term $\frac{1}{2} a^* f(x_0)$, then the flipping operation converges to the solution in one step (at first order):

$$\mathbf{P}_m [\rho + \frac{1}{2} a \delta(x - x_0) + \frac{1}{2} a^* f(x_0)] = \rho + O(a^2) \quad (\text{A4})$$

Although this result describes only local convergence, it shows how a few wrong peaks can be recovered easily.

References

1. L. Pauling and M. D. Shappell, *Zeits. f. Krist.* **75**, 128 (1930).
2. J.D. Bernal, I. Fankuchen, M. F. Perutz, ‘‘An X-Ray Study of Chymotrypsin and Haemoglobin.’’ *Nature* **141**, 523-524 (1938).
3. D. Sayre, ‘‘On the implication of a theorem due to Shannon’’, *Acta Cryst.* **5**, (1952) 843.
4. Y. M. Bruck and L. G. Sodin. ‘‘On the ambiguity of the image reconstruction problem.’’ *Optics Communications*, **30**(3):304-308, (1979).
5. R. Bates. ‘‘Fourier phase problems are uniquely solvable in more than one dimension. I: Underlying theory’’ *Optik*, **61**(3):247-262, 1982.
6. M. H. Hayes, ‘‘The reconstruction of a multidimensional sequence from the phase or magnitude of its Fourier transform,’’ *IEEE Trans. ASSP* **30**(2), 140-154, (1982).
7. M. H. Hayes and J. H. McClellan, ‘‘Reducible polynomials in more than one variable,’’ *Proc. IEEE* **70**(2), 197-198, (1982).
8. J. Miao, P. Charalambous, J. Kirz, D. Sayre, ‘‘Extending the methodology of X-ray crystallography to allow imaging of micrometre-sized non-crystalline specimens,’’ *Nature* **400**, 342-344 (1999).
9. D. Shapiro, P. Thibault, T. Beetz, V. Elser, M. Howells, C. Jacobsen, J. Kirz, E. Lima, H. Miao, A. Neiman, D. Sayre, ‘‘Biological imaging by soft x-ray diffraction microscopy,’’ *Proc. Nat. Acc. Sci.* **102**, 1543-1546 (2005). *Nature* **442**, 63-67 (2006).

10. A. Barty, S. Marchesini, H. N. Chapman, C. Cui, M. R. Howells, D. A. Shapiro, A. M. Minor, J. C. H. Spence, U. Weierstall, J. Ilavsky, A. Noy, S. P. Hau-Riege, A. B. Artyukhin, T. Baumann, T. Willey, J. Stolken, T. van Buuren, J. H. Kinney, "Three-dimensional coherent X-ray diffraction imaging of a ceramic nanofoam: determination of structural deformation mechanisms," *Phys. Rev. Lett.* **101**, 055501 (2008), [arXiv:0708.4035].
11. P. W. Hawkes & J. C. H. Spence (Eds.), *Science of Microscopy* (Springer, 2007).
12. E. J. Candès, J. Romberg and T. Tao, "Robust uncertainty principles: exact signal reconstruction from highly incomplete frequency information," *IEEE Trans. Inform. Theory*, **52**, 489-509 (2006) [arXiv:math/0409186].
13. M. L. Moravec, J. K. Romberg, R. G. Baraniuk, Richard, Compressive phase retrieval, *Wavelets XII. Proc. SPIE* **6701**, 670120 (2007).
14. E. van den Berg and M. P. Friedlander, SPGL1: A solver for large-scale sparse reconstruction, <http://www.cs.ubc.ca/labs/scl/index.php/Main/Spgl1>
15. E. van den Berg and M. P. Friedlander, "Probing the Pareto frontier for basis pursuit solutions", UBC Computer Science Technical Report TR-2008-01, January 2008. Available at http://www.optimization-online.org/DB_F
16. W. H. Richardson, "Bayesian-Based Iterative Method of Image Restoration". *J. Opt. Soc. Am. A* **62**, 55-59 (1972).
17. L. B. Lucy, "An iterative technique for the rectification of observed distributions". *Astronomical Journal* textbf79 745-754 (1974).
18. J.R. Fienup, "Phase Retrieval for Undersampled Broadband Images," *J. Opt. Soc. Am. A* **16**, 1831-1839 (1999).
19. S. Marchesini, H. He, H. N. Chapman, S. P. Hau-Riege, A. Noy, M. R. Howells, U. Weierstall, J.C.H. Spence, "X-ray image reconstruction from a diffraction pattern alone," *Phys. Rev. B* **68**, 140101(R) 1-4, (2003), [arXiv:physics/0306174].
20. L. D. Marks, W. Sinkler and E. Landree, "A Feasible Set Approach to the Crystallographic Phase Problem", *Acta Cryst.* **A55**, 601-612 (1999).
21. J. R. Fienup, "Reconstruction of an Object from the Modulus of Its Fourier Transform," *Opt. Lett.* **3**, 27-29 (1978).
22. J. R. Fienup, "Phase retrieval algorithms: a comparison", *Appl. Opt.* **21**, 2758-2769 (1982).
23. J. P. Abrahams, A. W. G. Leslie, *Acta Cryst.* **52**, 30-42 (1996).
24. V. Elser, "Phase retrieval by iterated projections," *J. Opt. Soc. Am. A* **20**, 40-55 (2003).
25. H. H. Bauschke, P. L. Combettes, and D. R. Luke, "Hybrid projection reflection method for phase retrieval," *J. Opt. Soc. Am. A* **20**, 1025-1034 (2003).
26. D. R. Luke, "Relaxed Averaged Alternating Reflections for Diffraction Imaging," *Inverse Problems* **21**, 37-50 (2005)., (arXiv:math.OC/0405208).
27. P. L. Combettes, "The Convex Feasibility Problem in Image Recovery, in *Advances in Imaging and Electron Physics*," (P. Hawkes, Ed.), vol. 95, pp. 155-270. (Academic Press, New York 1996).
28. S. Marchesini, "A unified evaluation of iterative projection algorithms for phase retrieval," *Rev. Sci. Inst.* **78**, 011301 1-10 (2007), [arXiv:physics/0603201].
29. G. Oszlányi and A. Süto, "Ab initio structure solution by charge flipping," *Acta Cryst.* **A60**, 134-141 (2004) [arXiv:cond-mat/0308129].
30. J. Wu, K. Leinenweber, J. C. H. Spence, "Ab initio phasing of X-ray powder diffraction patterns by charge flipping," *Nature Materials* **5**, 647-652 (2006).
31. E. J. Candès, D. L. Donoho, "New tight frames of curvelets and optimal Representations of objects with piecewise C^2 singularities." *Comm. Pure Appl. Math.* **57**, 219-266 (2004).
32. S. Marchesini, *J. Opt. Soc. Am. A* **24**, 32890-3296 (2007), [arXiv:physics/0611233].
33. G. Oszlányi and A. Süto, "Ab initio structure solution by charge flipping. II. Use of weak reflections," *Acta Crystallogr.* **A61**, 147-152 (2005).
34. I. Daubechies, M. Defrise, and C. D. Mol, "An iterative thresholding algorithm for linear inverse problems with a sparsity constraint," *Comm. Pure Appl. Math.* **57**(11), 1413-1457, (2004).